URSI AP-RASC 2019, New Delhi, India, 09 - 15 March 2019

Development of a method for estimating field map in an object containing magnetic materials from View Line Sequence in MRI

Shuang Liu* (1), Wenqi Qiu(1), Gabriel Della-Maggiora (2), Akihiro Kuwahata(1), Moriaki Kusakabe(3), Pablo Irarrazaval(2), Masaki Sekino(1)
(1) The University of Tokyo, Department of Electrical Engineering, Japan
(2) Pontifical Catholic University of Chile, Chile
(3) The University of Tokyo, Faculty and Graduate School of Agriculture and Life Science, Japan

Abstract

The inhomogeneous magnetic field distribution obtained in MRI is called Field Map. For some magnetic substances, such as iron-containing nanoparticles, the magnetic fields generated by these magnetic particles are too strong, which leads to the failure of conventional field map methods. A novel reconstruct method from View Line sequence image obtaining a field map has been proposed, after interpolation of undersampled discrete data points, the field map estimation of strongly inhomogeneous fields under simulation and real MRI data have been verified.

1. Introduction

In 1977, SLNB(Sentinel Lymph Node Biopsy) was first reported to be applied in a penile cancer treatment[1], After that, applied SLNB with injected radiotracer using the gamma probe in the treatment of breast cancer in 1993[2]. In recent years, in order to overcome the drawbacks of the SLNB in breast cancer treatment using the dye method[3] and the RI (Radioisotope) method[2], the SLNB based on detection of magnetic tracers like SPIONs (superparamagnetic iron oxide nanoparticles) is proposed[4][5]. These SPIONs such as Resovist (FUJIFILM RI Phama Co., Ltd.) with core sizes of 3–6 nm and carboxydextran coating (with 45–60 nm hydrodynamic sizes) can also be used in other fields like MRI (Magnetic Resonance Imaging) contrast enhancement[6].

Techniques for quantifying SPIONs can benefit many clinic researches such as optimizing the protocol of SLNB based on SPIONs. By injection different amount of the tracer and uses MRI to observe the accumulation amount, the best injection amount can be found.

The vast majority of SPIONs-based MRI study rely on qualitative analysis of the surrounding region of SPIONs (eg.[7][8][9]), A few rexometry method for quantification of low concentration Fe in SPIONs with MRI(0.05mg/ml[10], 0.1mg/mL[11], 0.2mg/mL[12])have been explored. These rexometry methods cannot deal with such high concentration of Fe in SPIONs-based SLNB because strong background inhomogeneous field induced by SPIONs make signal significantly decay around the SPIONs.

MRI field map is a promising way for quantifying SPIONs. However, the conventional MRI method for field map based on GRE (Gradient Recall Echo) sequence also suffers from the strong inhomogeneous field. Therefore, the field map near the area with Resovist cannot be acquired. In order to solve this problem, we propose a method named View Line based on Spin Echo which is able to avoid the large void signal area and generate the field map around the Resovist, so that provides more information than the conversational method based on Gradient Echo Sequence, However, this View Line sequence suffered from complicated reconstruction algorithm from images.

The goal of this paper is to demonstrate the applicability of estimating field map from images obtained by View Line Sequence in MRI.

2. View Line Sequence in MRI

2.1 Principle of View Line Sequence

The sequence diagram is shown in Fig. 1. This method can mainly divide into three parts. Part 1 is a normal slice selection part, part 2 achieves Line selection, part 3 is the readout module.

View Line sequence basically is modified from spin echo sequence, unlike SEMAC[13], this sequence did not encode slice distortion but extract this distortion information directly.

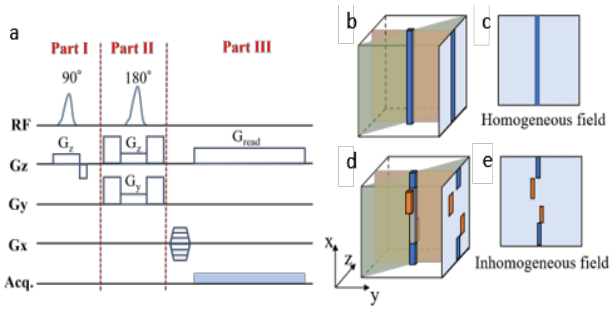

Figure 1 Diagram of View Line sequence (a) is the timing diagram of View Line sequence. (b-c) are examples of a sample and its acquired images under the homogeneous field, (d-e) represent line image acquired inhomogeneous background field in the z-direction. Orange and green planes in the cubic represent the actual position excited by 90 deg RF pulse and 180 rf pulse respectively.

2.2 Images obtained by View Line Sequence

Images obtained by View Line Sequence is shown in Fig.2. The excitation profile has been shown here, this image is a a vertical section of the sample, and the positive direction of main magnetic field in MRI (3T or 7T) is from 0 to 255 in vertical, under the high main magnetic field in MRI, magnetic material will be saturated. For undiluted Resoviost, the magnetic field generated is greater than the maximum range of slice selection RF frequency range, so there are black region in the image center which means the void signal.

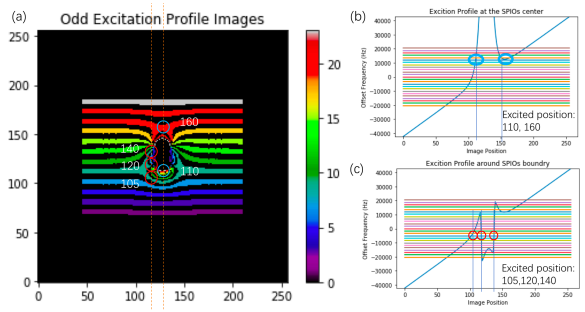

Figure 2 Diagram of excited lines by View Line Sequence with magnetic material (654 ug of iron generates a maximum magnetic field of approximately 1500 uT[5]) inside a water-contained sample (a) different colors represent the lines excited under different frequency of RF pulse (b) represent the center of the magnetic material with maximum positive magnetic field along with z-direction, (c) represent the position with maximum negative magnetic field generated by magnetic material.

3.Reconstruct Method

3.1 Preprocessing method

In order to extract the inhomogeneous magnetic field information, first we suppose the region outside the dark region is homogeneous, this is a reasonable assumption as the magnetic material would have induced much stronger magnetic field than normal tissues or sample. Under this assumption, we can skeletonize the line image, in Fig.3 shows the basic preprocessing method. Skeletonize can extract the rough information of inhomogeneous magnetic field, however, this method is not suitable for multi-objects. An improved preprocessing method has been proposed, it includes two parts, the proposed method is shown in Fig. 4. There are two parts of this method, one is the baseline detection, which can also be used for multi objects, and the distortion area detecting can obtain a range of distortion, by this information, we can restrict the processing region in MRI image, and the preprocessed image for line field map has been shown in fig.5. As it's shown, a narrow region has been obtained.

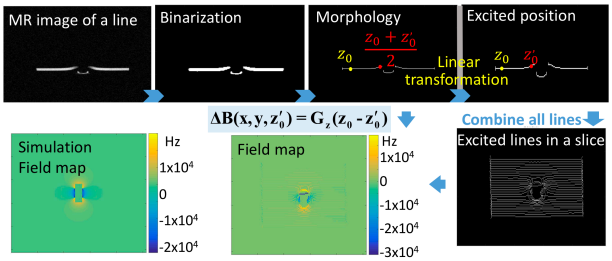

Figure 3 Diagram of basic preprocessing method, From left to right is origin MRI image, Binarization Image, Skeletonized Image, as the distance between inhomogenous curve to homogenous line depends on parameter setting for View Line sequence, here we need linear transformation to obtain actual excited position, finally by combing these line images, we can get the estimate line field map.

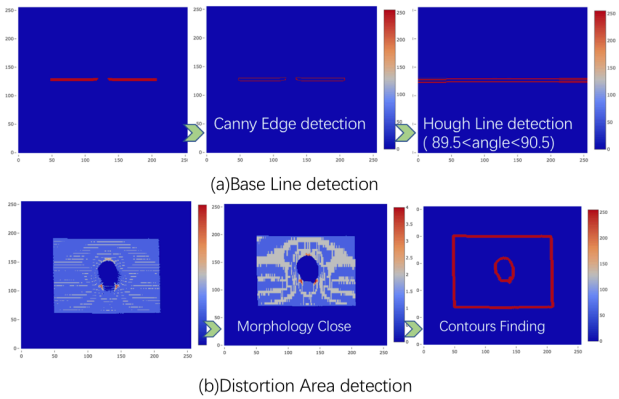

Figure 4 Diagram of proposed preprocessing method, (a) represents the baseline detection algorithm, which use the hough line detection technical, (b)represent the void signal region finding detection method, which used the contours finding method.

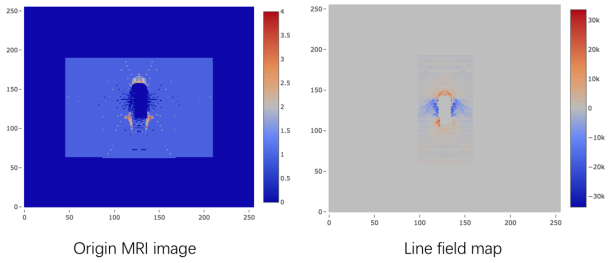

Figure 5 Diagram of line field map after preprocessing.

3.2 Interpolation method based on RBF

RBF is radial basis function, which is s a real-valued function whose value depends only on the distance from the origin, and it has been used a lot in interpolation.

Also in the field map estimating problem from View Line sequence, the RBF can be used as a powerful tool. In this work, we tested six forms RBF, as shown in Table 1, Because of the asymmetry of the data points of the line image, the main idea is that the 2D RBF function cannot be used, but the RBF interpolation should be performed for each vertical column. We evaluate the MSE(Mean Square Error) $\frac{1}{N}\sum_{i=1}^{N}\left(y_{i_{predict}} - y_{i_{target}}\right)^2$ of interpolated data to simulation target data. The evaluated result is shown in fig.6. with this evaluate graph, linear and multiquadric function has been selected, and find with multiquadric and smoothness parameter 2, shape parameter in the vertical set to 2, and shape parameter in horizontal direction give the least mean square error and enough smoothness. The final RBF interpolation for one column in field map is shown fig. 7.

Table 1 RBF tested in interpolation experiment

RBF name	form
Multiquadric	$\sqrt{1+\left(\frac{r}{\epsilon}\right)^2}$
Inverse	$1/\sqrt{1+\left(\frac{r}{\epsilon}\right)^2}$
Gaussian	$e^{-\left(\frac{r}{\epsilon}\right)^2}$
Linear	r
Cubic	r^3
Thin plate	$r^2\,log(r)$

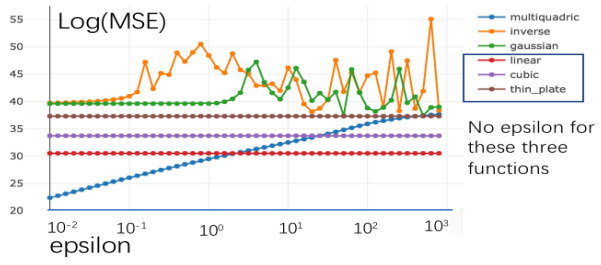

Figure 6 Diagram log(MSE) to shape parameter epsilon

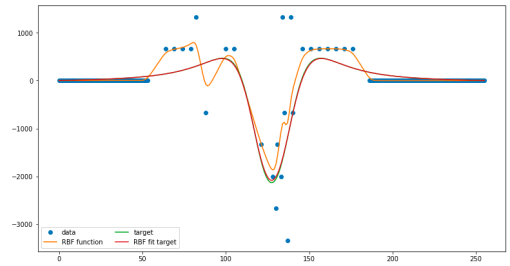

Figure 7 Diagram of multiquadric rbf fitting with one verticle line, blue dot points indicate the line field map data, the green line indicates the target simulation result, the orange line indicates the RBF interpolation result.

4. Verify experiment

During verify experiment, we use the sample shown in Fig.8, and the concentration and amount of Fe is shown in Table 2. Sample one is the undiluted Resovist, and sample 2 to 5 are the products of sample 1 after the corresponding dilution rate. Sample one has been saturated in MRI (Bruker 7T animal MRI), whose magnetic moment measured by SQUID is $2.08 * 10^{-5}\mathrm{Am}^2$[5], and the magnetic moment is proportional to the amount of Fe.

Each sample has been verified in both artificial data and real MRI data, the interpolated image result is shown in Fig.9. The left side is the real MRI data, and the right side is the artificial simulation data. When comparing these two-type result, the max value of field map from MRI image is smaller than max value of field map from the simulation.

Table 2. Concentration and amount of Fe in each sample.

Sample number	Concentration of Fe (g/L)	Amount of Fe (μg)
1	27.9	654
2	13.9	327
3	7.0	163
4	3.5	82
5	1.7	41

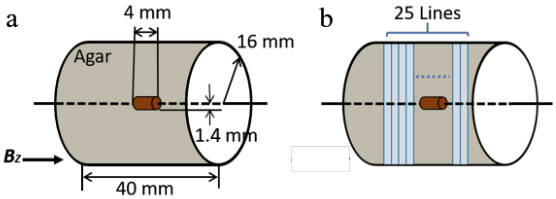

Figure 8 Sample we used in the experiment(a) A diagram of a sample. The brown cylinder represents the SPION container, and agar is filled in the larger container with yellow color. Excited positions are shown in (b) as blue lines.

5. Summary

After this preprocessing and interpolation algorithm, the field map from view line sequence can be obtained even under low concentration. This algorithm works well for high concentration because of the much obvious distortion in MRI image.

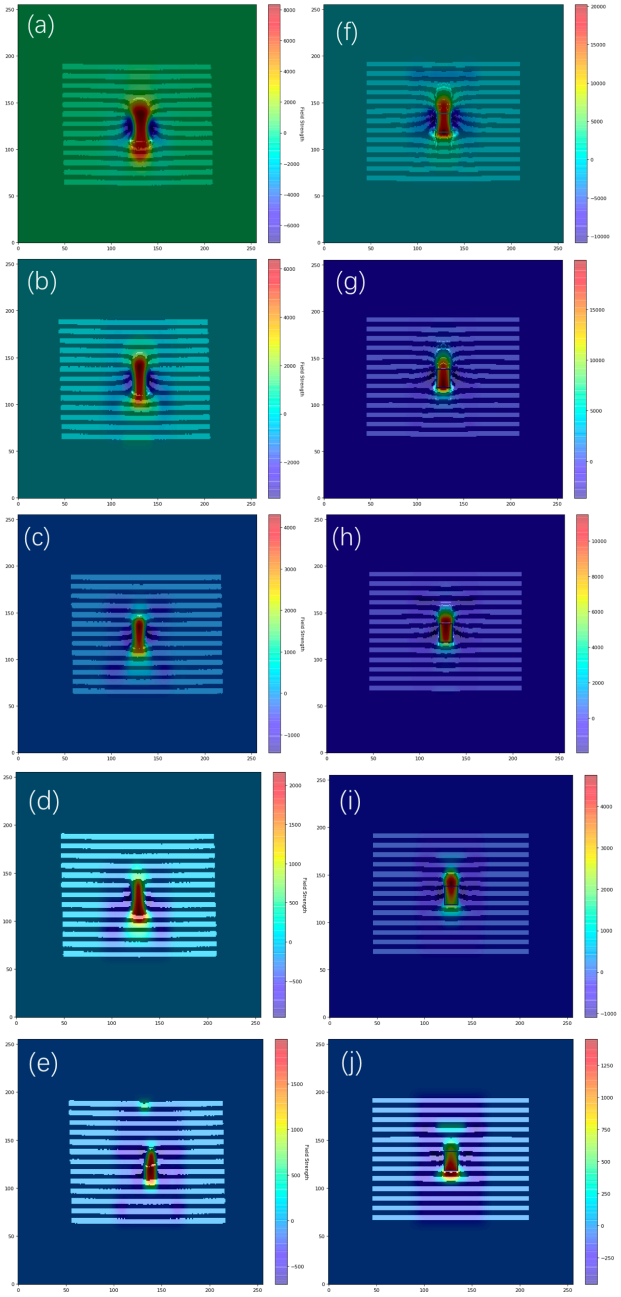

Figure 9 Diagram of interpolation result for real MRI result (a-e), and artifical data (f-j) for constration in table 2.

6. References

[1] R. M. Cabanas, "An approach for the treatment of penile carcinoma," *Cancer*, vol. 39, no. 2, pp. 456–466, Feb. 1977.

[2] D. N. Krag, D. L. Weaver, J. C. Alex, and J. T. Fairbank, "Surgical resection and radiolocalization of the sentinel lymph node in breast cancer using a gamma probe.," *Surg. Oncol.*, vol. 2, no. 6, p. 335–9; discussion 340, Dec. 1993.

[3] A. S. ROSS and C. D. SCHMULTS, "Sentinel Lymph Node Biopsy in Cutaneous Squamous Cell Carcinoma: A Systematic Review of the English Literature," *Dermatologic Surg.*, vol. 32, no. 11, pp. 1309–1321, Nov. 2006.

[4] A. Kuwahata, S. Chikaki, A. Ergin, M. Kaneko, M. Kusakabe, and M. Sekino, "Three-dimensional sensitivity mapping of a handheld magnetic probe for sentinel lymph node biopsy," *AIP Adv.*, vol. 7, no. 5, p. 056720, May 2017.

[5] M. Sekino *et al.*, "Handheld magnetic probe with permanent magnet and Hall sensor for identifying sentinel lymph nodes in breast cancer patients," *Sci. Rep.*, vol. 8, no. 1, p. 1195, Dec. 2018.

[6] Y.-X. J. Wang, "Superparamagnetic iron oxide based MRI contrast agents: Current status of clinical application.," *Quant. Imaging Med. Surg.*, vol. 1, no. 1, pp. 35–40, Dec. 2011.

[7] R. Weissleder *et al.*, "In vivo magnetic resonance imaging of transgene expression.," *Nat. Med.*, vol. 6, no. 3, pp. 351–355, 2000.

[8] R. Guzman *et al.*, "Long-term monitoring of transplanted human neural stem cells in developmental and pathological contexts with MRI," vol. 104, no. 24, pp. 10211–10216, 2007.

[9] M. Zhao, D. A. D. A. a Beauregard, L. Loizou, B. Davletov, and K. M. M. K. M. Brindle, "Non-invasive detection of apoptosis using magnetic resonance imaging and a targeted contrast agent.," *Nat. Med.*, vol. 7, pp. 1241–1244, 2001.

[10] A. M. Rad, A. S. Arbab, Q. Jiang, and H. Soltanian-zadeh, "Quantification of Superparamagnetic Iron Oxide (SPIO)-labeled Cells Using MRI," vol. 26, no. 2, pp. 366–374, 2007.

[11] W. Liu, H. Dahnke, J. Rahmer, E. K. Jordan, and J. A. Frank, "Ultrashort T 2* relaxometry for quantitation of highly concentrated superparamagnetic iron oxide (SPIO) nanoparticle labeled cells," *Magn. Reson. Med.*, vol. 61, no. 4, pp. 761–766, 2009.

[12] N. A. Pelot and C. V. Bowen, "Quantification of superparamagnetic iron oxide using inversion recovery balanced steady-state free precession," *Magn. Reson. Imaging*, vol. 31, no. 6, pp. 953–960, 2013.

[13] W. Lu, K. B. Pauly, G. E. Gold, J. M. Pauly, and B. a Hargreaves, "SEMAC: Slice Encoding for Metal Artifact Correction in MRI.," *Magn. Reson. Med.*, vol. 62, no. 1, pp. 66–76, 2009.